

# Band Electronic Structure of One- and Two-Dimensional Pentacene Molecular Crystals<sup>†</sup>

R. C. Haddon,\*<sup>‡</sup> X. Chi,<sup>‡</sup> M. E. Itkis,<sup>‡</sup> J. E. Anthony,<sup>§</sup> D. L. Eaton,<sup>§</sup> T. Siegrist,<sup>||</sup>  
C. C. Mattheus,<sup>⊥</sup> and T. T. M. Palstra<sup>⊥</sup>

Departments of Chemistry and Chemical & Environmental Engineering, University of California, Riverside, California 92521-0403, Department of Chemistry, Advanced Carbon Materials Center, University of Kentucky, Lexington, Kentucky 40506-0055, Bell Laboratories, Lucent Technologies, Murray Hill, New Jersey 07974, Department of Materials Chemistry, P.O. Box 124, Lund University, 221 00 Lund, Sweden, and Solid State Chemistry Laboratory, Materials Science Center, University of Groningen, The Netherlands

Received: March 22, 2002; In Final Form: June 6, 2002

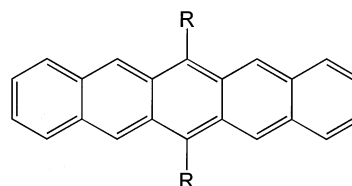
We report EHT calculations of the band electronic structure of substituted pentacene derivatives and the polymorphs of the parent compound. The results show that there are wide disparities among the bandwidths and electronic dimensionalities of these compounds. The parent pentacene polymorphs are 2-dimensional in their band electronic structure with moderate dispersions; the bandwidths in the 14.1 Å d-spacing polymorph are noticeably larger than for the 14.5 Å d-spacing polymorph, reported by Campbell. Whereas the parent pentacene polymorphs adopt the well-known herringbone packing, the new, substituted pentacenes are noticeably different in their solid state structures and this is reflected in the band electronic structures. TMS adopts a highly 1-dimensional structure that leads to a large bandwidth along the stacking direction; TIPS also adopts a stacked structure, but because the molecules are laterally interleaved in the fashion of bricks in a wall, this compound is strongly 2-dimensional.

## Introduction

Rigorously purified single crystals of pentacene show high mobilities at low temperature, and this result has been interpreted in terms of band transport.<sup>16</sup> It is fundamental to our understanding of transport processes in solid-state materials that conductivity comes about as result of a conducting pathway and the availability of carriers (electrons or holes). It is important to note that this understanding of the relationship between conductivity and orbital overlap is not necessarily based on sophisticated theories of electronic structure, but is usually made obvious in the simplest methods, such as the Extended Huckel Theory (EHT);<sup>14</sup> It is for this reason that EHT band structure calculations have been widely used in the rationalization of the electronic structure of organic conductors and superconductors.

In a recent article on pentacene, it was shown that the single crystals exhibit high field effect mobilities.<sup>19</sup> Not all polymorphs can be grown as single crystals, and in the thin films the mobility is limited by grain boundaries. We compared the 14.1 Å d-spacing polymorph<sup>19–21</sup> with the 14.5 Å d-spacing polymorph reported by Campbell.<sup>22</sup> In the present article, we use extended Huckel theory (EHT) calculations of the valence and conduction bands to show that the interactions between neighboring organic molecules in the crystal lattice are dominated by their orientation and arrangement rather than by their interatomic separations.<sup>3</sup> We also report the band electronic structure of two new

pentacene derivatives that are forced into stacking geometries by the attachment of substituents to the pentacene molecule.<sup>1</sup>



R = H (pentacene)

R = C≡C—Si(CH<sub>3</sub>)<sub>3</sub> (TMS)

R = C≡C—Si(CH(CH<sub>3</sub>)<sub>2</sub>)<sub>2</sub> (TIPS)

In crystals of TMS, the molecules adopt a simple one-dimensional (1-D) stack that has short interatomic spacings (~3.4 Å) and excellent overlap along the stacking direction. In crystals of TIPS, the molecules are also arranged in stacks, but there is a large offset in the arrangement so that each molecule overlaps above and below with two neighboring molecules in the stack; in this way, the molecules develop interactions lateral to the stacking direction. These two stacked structures found in the substituted pentacenes contrast with the herringbone structure of the unsubstituted pentacene polymorphs.<sup>19</sup>

For comparison purposes, we also include the band structure of solid C<sub>60</sub> although EHT calculations on K<sub>3</sub>C<sub>60</sub> have been reported previously.<sup>7,11</sup> At the EHT level of theory, there is little difference between the band structures of these two solids. Nevertheless, C<sub>60</sub> and C<sub>70</sub> are known to function as field effect transistors,<sup>10,8</sup> and recent work has shown that field effect doping of the parent fullerenes can induce superconductivity at low temperatures.<sup>15</sup> The previous EHT calculations on K<sub>3</sub>C<sub>60</sub> gave a bandwidth for the half-filled t<sub>1u</sub> level of 0.5 eV,<sup>11</sup> which may

<sup>†</sup> Part of the special issue "John C. Tully Festschrift".

\* To whom correspondence should be addressed.

<sup>‡</sup> Departments of Chemistry and Chemical & Environmental Engineering, University of California, Riverside.

<sup>§</sup> Department of Chemistry, Advanced Carbon Materials Center, University of Kentucky.

<sup>||</sup> Bell Laboratories, Lucent Technologies and Department of Materials Chemistry, Lund University.

<sup>⊥</sup> University of Groningen.

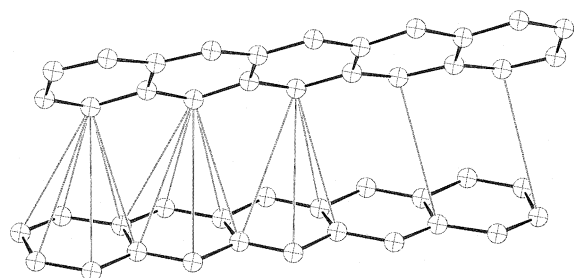


**Figure 1.** View of the herringbone structure of 14.5-pentacene, showing intermolecular contacts that fall within 4 Å. This arbitrary value was chosen to accentuate the differences between polymorphs.

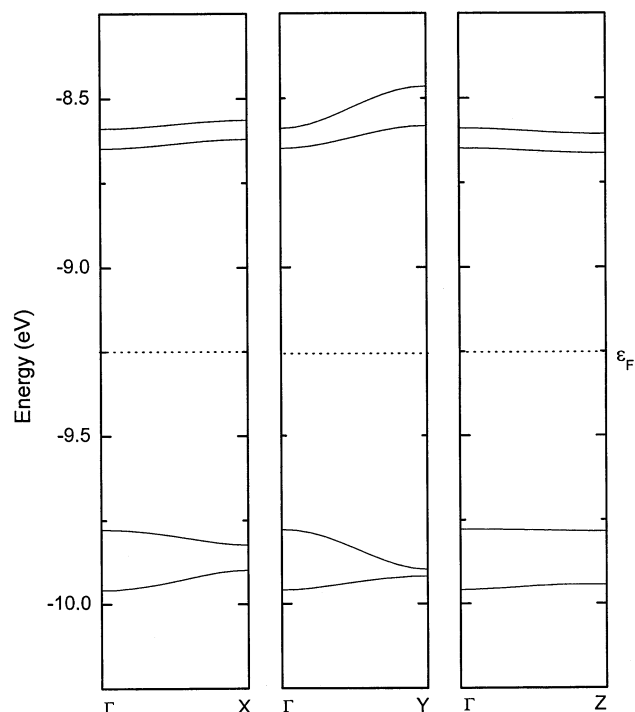


**Figure 2.** Electronic structure of the valence and conduction bands of 14.5-pentacene along X (a\*), Y (b\*), and Z (c\*).

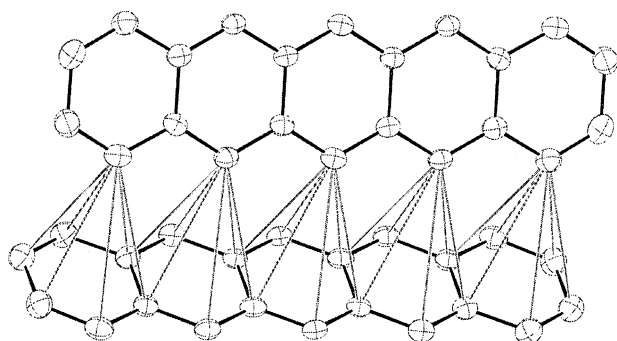


**Figure 3.** View of the herringbone structure of 14.1-pentacene, showing intermolecular contacts that fall within 4 Å (see Figure 1).

be compared with the bandwidth of 0.6 eV obtained by LDA calculations.<sup>6</sup>

## Results and Discussion

The structures and calculated valence and conduction bands for the parent pentacene polymorphs are shown in Figures 1–4. In the solid state, there are two molecules in the asymmetric units of both cells, and thus there is a pair of energy bands for the valence and conduction bands. The energy bands of both

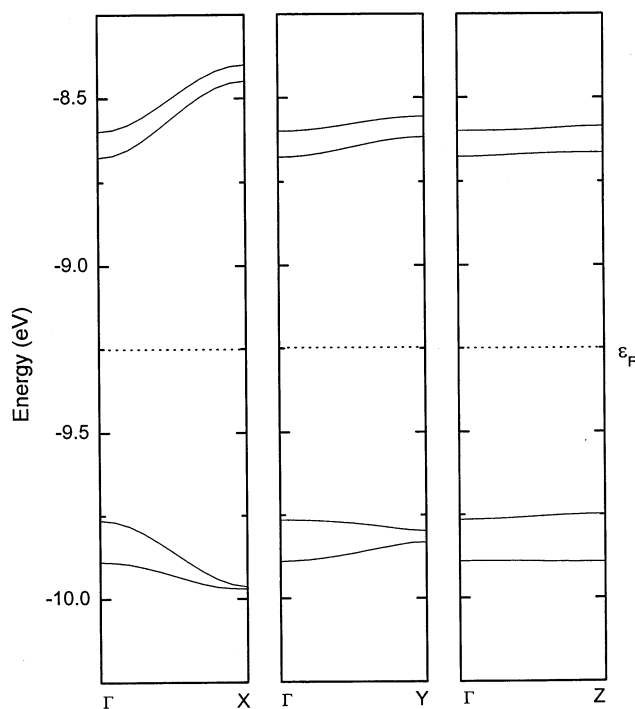


**Figure 4.** Electronic structure of the valence and conduction bands of 14.1-pentacene along X (a\*), Y (b\*), and Z (c\*).

**TABLE 1: Band Dispersions for Pentacenes**

compd	direction	conduction band <sup>a</sup> (eV)	valence band <sup>a</sup> (eV)
14.5-pentacene	X	0.03, 0.03 (0.08)	0.05, 0.06 (0.18)
	Y	0.12, 0.07 (0.18)	0.12, 0.04 (0.18)
	Z	0.03, 0.02 (0.07)	0.01, 0.02 (0.18)
14.1-pentacene	X	0.22, 0.20 (0.28)	0.20, 0.08 (0.21)
	Y	0.06, 0.04 (0.12)	0.06, 0.03 (0.13)
	Z	0.01, 0.01 (0.09)	0.02, 0.00 (0.13)
TMS	X	0.86	0.09
	Y	0.02	0.03
	Z	0.01	0.01
TIPS	X	0.36	0.15
	Y	0.33	0.03
	Z	0.00	0.00
C <sub>60</sub>	X	0.53 (t <sub>1u</sub> ), 0.60 (t <sub>1g</sub> )	0.61 (h <sub>u</sub> )

<sup>a</sup> The values in parentheses refer to the total width of the band complex for both pentacene molecules in the asymmetric unit. In the case of C<sub>60</sub>, the values given are for the total bandwidth of orbitals that are degenerate in the free molecule.

polymorphs display appreciable dispersion along X (a\*) and Y (b\*), and thus, they reflect the herringbone stacking arrangement found previously in the crystal structures and indicate a 2-D electronic structure for these materials.

The band dispersions of all of the pentacenes are summarized in Table 1, where it may be seen that the valence band dispersions of the 14.1 Å d-spacing polymorph (14.1-pentacene) are calculated to be greater than the values obtained for the 14.5 Å d-spacing polymorph (14.5-pentacene), in agreement with the superior physical properties found for this polymorph.<sup>19</sup> The dispersion in the highest lying valence band of 14.1-pentacene is calculated to be about 0.2 eV along the X direction, whereas space charge limited spectroscopy gives an effective in-plane bandwidth for hole conduction of 0.1–0.4 eV in the temperature range 300 to 10 K.<sup>16</sup>

Our results may be compared with recent INDO calculations on 14.1-pentacene clusters.<sup>5</sup> These calculations obtain a splitting of the energy levels for the two molecules in the unit cell of

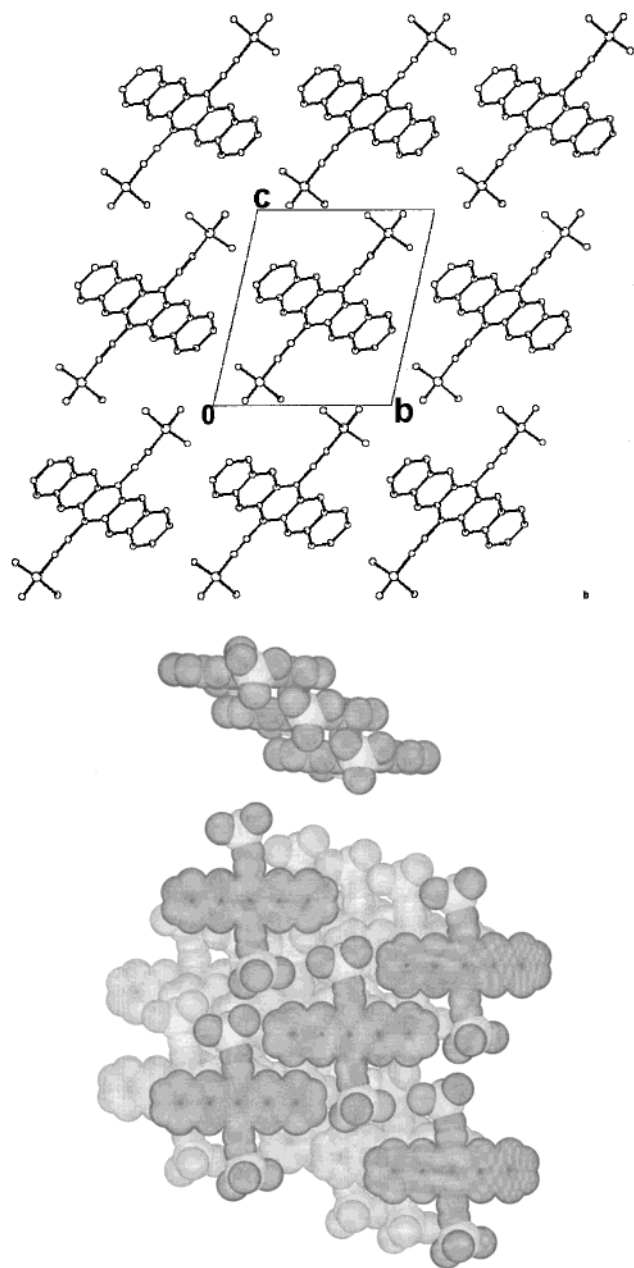


**Figure 5.** View down the crystallographic *a* axis, showing isolated columns of  $\pi$ -stacked TMS molecules together with space filling views of the crystal packing.

0.061 eV (HOMO) and 0.070 eV (LUMO),<sup>5</sup> which may be compared with the values obtained with EHT theory of 0.020 and 0.033 eV, respectively. The INDO calculations<sup>5</sup> provide estimates of 0.61 and 0.59 eV for the conduction and valence bandwidths, respectively. Thus, the INDO calculations give interaction energies in the crystal lattice that are 2 to 3 times larger than the EHT calculations.

Our analysis supports previous work<sup>17,18,12,5,3</sup> which suggests that carbon-carbon interactions are surprisingly effective even when the interactions occur at distances that far exceed the sum of the van der Waals separations (3.4 Å) and do not involve the type of head-on  $\pi$ -orbital overlap that occurs in crystalline  $C_{60}$ . Relatively weak interactions between carbon-based  $p\pi$ -systems (Table 1), are shown to be capable of supporting high conductivities that probably involve band transport.<sup>2,16</sup>

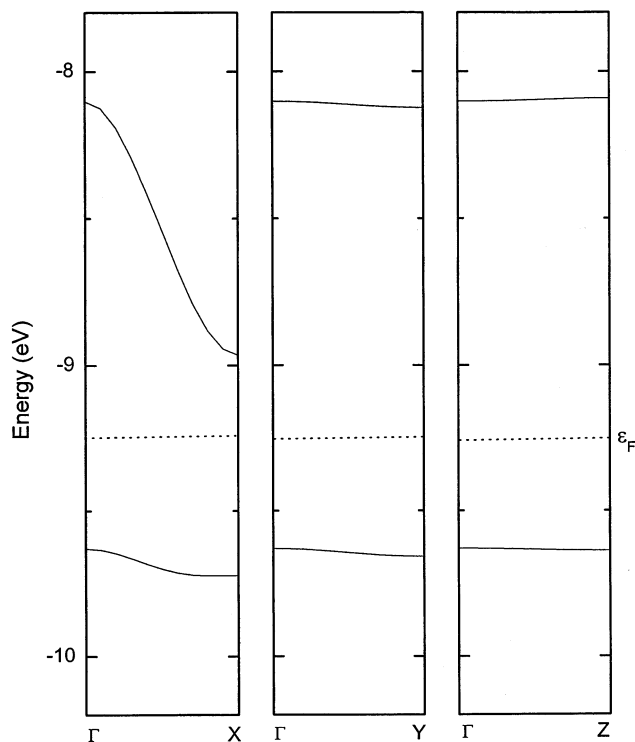


**Figure 6.** Electronic structure of the valence and conduction bands of TMS along X (*a\**), Y (*b\**), and Z (*c\**).

In contrast to the pentacene polymorphs, the substituted pentacene derivatives adopt stacked structures (Figures 5 and 7), and this is reflected in the highly anisotropic band electronic structure (Figures 6 and 8). Of most note, however, is the large dispersion in the conduction bands (Table 1); this amounts to about 0.9 eV in TMS and 0.7 eV in TIPS and is to be expected given the close approach between the stacked molecular planes which are reported to be at the van der Waals separation for pairs of carbon atoms.<sup>1</sup>

TMS adopts a slipped 1-D stacking arrangement which superimposes slightly less than four out of the five benzene rings in the pentacene structure at distances close to the van der Waals separations for pairs of carbon atoms (3.4 Å). As a result the bandwidth of the conduction band (0.9 eV) is unprecedented for a neutral molecular crystal, and exceeds even that of  $C_{60}$ , which has intermolecular carbon-carbon distances of 3.3 Å; nevertheless,  $C_{60}$  is face-centered cubic with overlap in 3-dimensions rather than being confined to a single direction as is found in TMS (see Figure 9).

TIPS also adopts a stacked structure, but the details are unusual (Figure 7). The TIPS structure is composed of interleaved molecular plates, in just the same way that bricks are laid and produces a wall of molecules connected in 2-D. Presumably to avoid the bulky central groups, the surface of any given pentacene overlaps with two other pentacenes in the stacks so that about two benzene rings in a pair of pentacenes actually overlap. Because any pentacene overlaps with two molecules in the stack (both above and below), a lateral conducting pathway is established. The stacking axis is approximately along Y and the lateral direction lies approximately along X. It may be seen that the conduction band shows similar dispersion along these two directions [0.33 eV (stacking direction), 0.36 eV (lateral direction)], but the valence band exhibits significantly greater dispersion along the X direction [0.03 eV (stacking direction), 0.15 eV (lateral direction)].

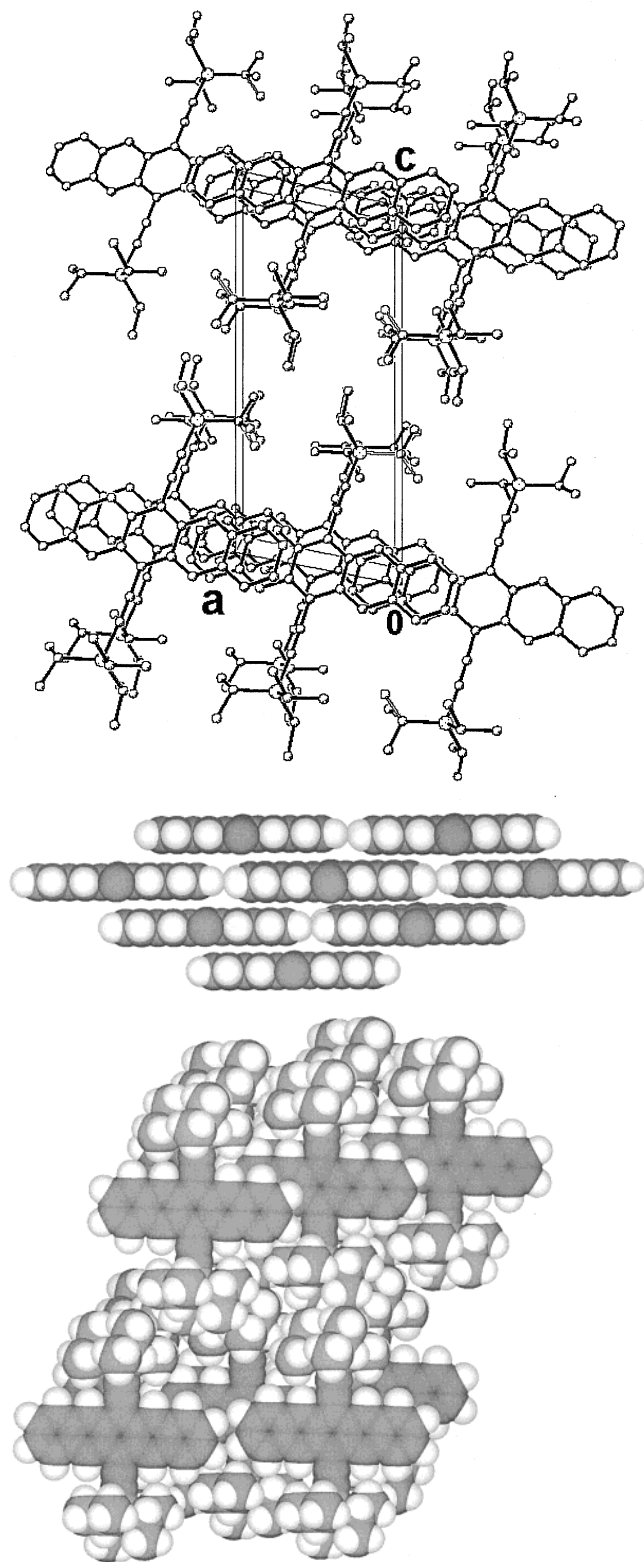


**Figure 7.** View down the crystallographic  $b$  axis, corresponding to the  $\pi$ -stacking axis, showing two-dimensional stacks of TIPS molecules together with space filling views of the crystal packing.

### Conclusion

There are wide disparities among the bandwidths and electronic dimensionalities of the pentacene molecular crystals discussed in the present report. The parent pentacene polymorphs are 2-D in their electronic structure with moderate dispersions; the bandwidths in the vapor phase grown material are noticeably larger than those in the solution phase material. The dispersions

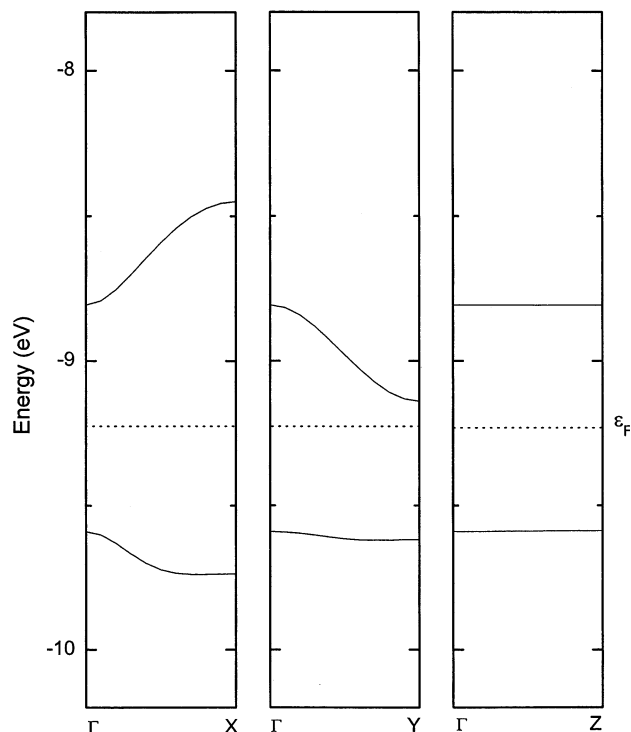


**Figure 8.** Electronic structure of the valence and conduction bands of TIPS along X ( $a^*$ ), Y ( $b^*$ ), and Z ( $c^*$ ).

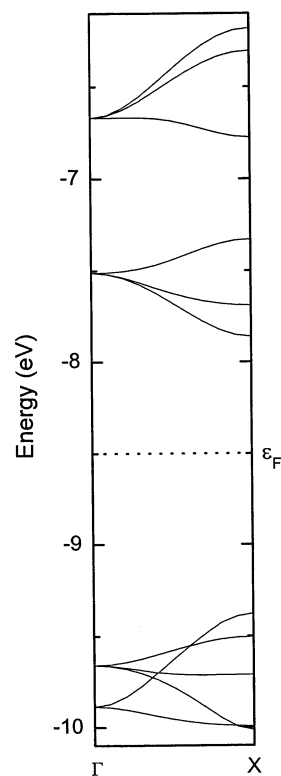


**Figure 9.** Electronic structure of the valence and conduction bands of  $C_{60}$  along X.

in the valence bands are calculated to be: 0.05 (X), 0.12 eV (Y) 14.5-pentacene; 0.20 (X), 0.06 eV (Y) 14.1-pentacene. Whereas the parent pentacene polymorphs adopt the well-known herringbone packing, the new substituted pentacenes are noticeably different in their crystal packing structures. TMS adopts a highly 1-D structure that leads to a large bandwidth along the stacking direction (X); TIPS also adopts a stacked structure (Y),



but because the molecules are laterally interleaved (along X) in the fashion of bricks in a wall, this compound is strongly 2-dimensional. The calculated dispersions in the valence bands: 0.09 (X), 0.03 eV (Y) TMS; 0.15 (X), 0.03 eV (Y) TIPS, are dwarfed by the dispersions in the conduction bands: 0.86 (X), 0.02 eV (Y) TMS; 0.36 (X), 0.33 eV (Y) TIPS.

### Experimental Section

**X-ray Crystallography.** Crystallographic data have been previously reported.<sup>1,19–22</sup> The coordinates from these structure determinations were used directly in the band structure calculations.

**Band Structure Calculations.** The band structure calculations made use of a modified version of the extended Hückel theory (EHT) band structure program originally supplied by M.-H. Whangbo. The parameter set is chosen to provide a reasonably consistent picture of bonding in heterocyclic organic compounds.<sup>4,12</sup> In the case of benzenoid hydrocarbons, EHT calculations are known to give  $\sigma$ -orbitals which lie too high in energy relative to the  $\pi$ -orbitals,<sup>13,9</sup> and in certain circumstances, the  $\sigma$ -orbitals are interspersed with the  $\pi$ -orbital manifold. We have neglected these  $\sigma$ -orbitals, and all of the crystal orbitals shown in the band diagrams have been confirmed to arise from  $\pi$ -orbitals.

**Acknowledgment.** This work was supported by the Office of Basic Energy Sciences, Department of Energy, under Grant No. DE-FG032-97ER45668 and by Los Alamos National Laboratories, Grant No. STB-UC:10019-001.

### References and Notes

- (1) Anthony, J. A.; Brooks, J. S.; Eaton, D. L.; Parkin, S. L. *J. Am. Chem. Soc.* **2001**, *123*, 9482–9483.
- (2) Chi, X.; Itkis, M. E.; Patrick, B. O.; Barclay, T. M.; Reed, R. W.; Oakley, R. T.; Cordes, A. W.; Haddon, R. C. *J. Am. Chem. Soc.* **1999**, *121*, 10 395–10 402.
- (3) Chi, X.; Itkis, M. E.; Reed, R. W.; Oakley, R. T.; Cordes, A. W.; Haddon, R. C. *J. Phys. Chem. B* **2002**, *106*, 8278–8287.
- (4) Cordes, A. W.; Haddon, R. C.; Oakley, R. T.; Schneemeyer, L. F.; Waszczak, J. V.; Young, K. M.; Zimmerman, N. M. *J. Am. Chem. Soc.* **1991**, *113*, 582.
- (5) Cornil, J.; Calbert, J. P.; Bredas, J. L. *J. Am. Chem. Soc.* **2001**, *123*, 1250–1251.
- (6) Erwin, S. C.; Pickett, W. E. *Science* **1991**, *254*, 842–845.
- (7) Haddon, R. C. *Acc. Chem. Res.* **1992**, *25*, 127.
- (8) Haddon, R. C. *J. Am. Chem. Soc.* **1996**, *118*, 3041–3042.
- (9) Haddon, R. C.; Hebard, A. F.; Rosseinsky, M. J.; Murphy, D. W.; Duclos, S. J.; Miller, B.; Fleming, R. M.; Siegrist, T.; Glarum, S. H.; Tycko, R. *ACS Symposium Series* **1992**, *481*, 71–89.
- (10) Haddon, R. C.; Perel, A. S.; Morris, R. C.; Palstra, T. T. M.; Hebard, A. F.; Fleming, R. M. *Appl. Phys. Lett.* **1995**, *67*, 121–123.
- (11) Haddon, R. C.; Ramirez, A. P.; Glarum, S. H. *Adv. Mater.* **1994**, *6*, 316–322.
- (12) Haddon, R. C.; Siegrist, T.; Fleming, R. M.; Bridenbaugh, P. M.; Laudise, R. A. *J. Mater. Chem.* **1995**, *5*, 1719–1724.
- (13) Hoffmann, R. *J. Chem. Phys.* **1963**, *39*, 1397–1412.
- (14) Hofmann, R. *Solids and Surfaces*; VCH: New York, 1988.
- (15) Schoen, J. H.; Kloc, C.; Haddon, R. C.; Batlogg, B. A Superconducting Field Effect Switch. *Science* **2000**, *288*, 656–658.
- (16) Schoen, J. H.; Kloc, C.; Batlogg, B. *Phys. Rev. Lett.* **2001**, *86*, 3843.
- (17) Siegrist, T.; Fleming, R. M.; Haddon, R. C.; Laudise, R. A.; Lovinger, A. J.; Katz, H. E.; Bridenbaugh, P.; Davis, D. D. *J. Mater. Res.* **1995**, *10*, 2170–2173.
- (18) Siegrist, T.; Kloc, C.; Laudise, R. A.; Katz, H. E.; Haddon, R. C. *Adv. Mater.* **1998**, *10*, 379–382.
- (19) Siegrist, T.; Kloc, C.; Schoen, J. H.; Batlogg, B.; Haddon, R. C.; Berg, S.; Thomas, G. A. *Angew. Chem., Int. Ed.* **2001**, *40*, 1732–1736.
- (20) Holmes, D.; Kumaraswamy, S.; Matzger, A. J.; Vollhardt, K. P. *C. Chem. Eur. J.* **1999**, *5*, 3399.
- (21) Mattheus, C. C.; Dros, A. B.; Baas, J.; Meetsma, A.; de Boer, J. L.; Palstra, T. T. M. *Acta Crystallogr.* **2001**, *C57*, 939.
- (22) Campbell, R. B.; Robertson, J. M.; Trotter, J. *Acta Crystallogr.* **1961**, *14*, 705.